FEBS Letters 580 (2006) 67–71

Differences in catalytic activity between rat testicular and ovarian carbonyl reductases are due to two amino acids

Michel A. Sciotti[a], Steven Tam[b], Bendicht Wermuth[a,*], Michael E. Baker[b,*]

[a] *Institute of Clinical Chemistry, 3010 Bern, Switzerland*
[b] *Department of Medicine, 0693 University of California, San Diego, 9500 Gilman Drive, La Jolla, CA 92093-0693, USA*

Received 7 September 2005; revised 26 October 2005; accepted 15 November 2005

Available online 6 December 2005

Edited by Miguel De la Rosa

Abstract The sequences of rat testis carbonyl reductase (rCR1) and rat ovary carbonyl reductase (rCR2) are 98% identical, differing only at amino acids 140, 141, 143, 235 and 238. Despite such strong sequence identity, we find that rCR1 and rCR2 have different catalytic constants for metabolism of menadione and 4-benzoyl-pyridine. Compared to rCR1, rCR2 has a 20-fold lower K_m and 5-fold lower k_{cat} towards menadione and a 7-fold lower K_m and 7-fold lower k_{cat} towards 4-benzoyl-pyridine. We constructed hybrids of rCR1 and rCR2 that were changed at either residues 140, 141 and 143 or residues 235 and 238. rCR1 with residues 140, 141 and 143 of rCR2 has similar catalytic efficiency for menadione and 4-benzoyl-pyridine as rCR1. rCR1 with Thr-235 and Glu-238 of rCR2 has the catalytic constants of rCR2, indicating that it is this part of rCR2 that contributes to its lower K_m for menadione and 4-benzoyl-pyridine. Comparisons of three-dimensional models of rCR1 and rCR2 show how Thr-235 and Glu-238 stabilize rCR2 binding of NADPH and menadione.

Keywords: Carbonyl reductase; Enzyme evolution; Xenobiotics

1. Introduction

Carbonyl reductase (CR) catalyses the NADPH-dependent reduction of various endogenous carbonyl compounds and androgens [1–5]. CR belongs to the short-chain dehydrogenases/reductases (SDR) superfamily [6], a large family of enzymes that catalyze the oxidation or reduction of a wide variety of substrates, including steroids and prostaglandins [6,7].

In 1995, we determined the amino acid sequence of CR (rCR1) from rat testis [8] and found it to be about 80% identical to human CR [1]. Two years later, Aoki et al. [5] characterized a second rat CR (rCR2) from ovary that was inducible by pregnant mare serum gonadotropin. They did not express rCR2 and study its catalytic activity, which seemed unnecessary because the amino acid sequences of rCR1 and rCR2 are 98% identical; they differ in only five residues: 140, 141, 143, 235 and 238. With such strong similarity, it is reasonable to assume that rCR1 and rCR2 have similar enzymatic properties. However, the five differences are localized to two sites that have interesting functional properties. The amino acids at 140, 141, and 143 are close to the catalytically important serine-139 [6,9]. In rat CR1 and human CR, amino acid 238 is a lysine that is covalently modified by an autocatalytic reaction with 2-oxocarboxylates, such as pyruvate [4,10,11]. Lysine-238 is replaced with glutamic acid in rat CR2. The potential functional importance of these differences between rCR1 and rCR2 prompted us to investigate their catalytic properties in more detail.

Here we show that despite 98% amino acid identity between rCR1 and rCR2, they have different catalytic constants for menadione and 4-benzoyl-pyridine. By constructing hybrids that differ either at residues 140, 141 and 143 or at residues 235 and 238, we determined that Thr-235 and Glu-238 are responsible for the different catalytic properties of rCR1 and rCR2. Comparison of three-dimensional models of rCR1 and rCR2 with NADPH and menadione, which we constructed, indicates that Thr-235 has important stabilizing interactions with NADPH and menadione, and Glu-238 stabilizes Trp-229, which interacts with menadione. Our data show that rCR1 and rCR2 in testes and ovary, respectively, are an example of how small changes in amino acid can lead to the evolution of different catalytic constants in an enzyme.

2. Materials and methods

2.1. Materials

For mutagenesis and expression of rat CRs, we used *rcr*1 recombinant cDNA, subcloned into a pET-11 inducible expression vector from a λgt11 rat testis cDNA library as previously described [8]. Genomic rat DNA was prepared from male Sprague–Dawley rat blood.

2.2. Mutagenesis

rcr2 and mutant genes *rcr*1/2 and *rcr*2/1 were constructed by mutating the corresponding recombinant *rcr*1 cloned in pET11a by the Higuchi method [12]. *rcr*2/1 is a S140G, V141M, L143R mutant of *rcr*1. *rcr*1/2 is a A235T, K238E mutant of *rcr*1. We sequenced each mutant to verify that the only mutations were those at the desired amino acids in rCR.

PCR products obtained with the expand high fidelity PCR system were cloned into the PCR-product cloning vector pT-Adv. *rcr* mutants were digested by *Kpn*I and *Nco*I and inserted into recombinant *rcr*1 cloned in pET11a.

2.3. Recombinant gene expression and enzyme purification

Recombinant plasmids were transfected into *Escherichia coli* BL21 by electroporation and plated on LB agar containing 50 μg/ml ampicillin. A clone was cultured in LB containing 50 μg/ml ampicillin. Expression was induced by adding 0.4% IPTG to the culture. After 5 h, cells

*Corresponding authors. Fax: +41 31 632 4862 (B. Wermuth), +1 619 543 7069 (M.E. Baker).
E-mail addresses: Bendicht.Wermuth@insel.ch (B. Wermuth), mbaker@ucsd.edu (M.E. Baker).

0014-5793/$32.00
doi:10.1016/j.febslet.2005.11.049

were collected by centrifugation and resuspended in 20 ml of 10 mM Tris–HCl, pH 8.6, containing 1 mM EDTA and disrupted by freeze–thawing and sonication. The supernatant was treated with RNAses and DNAse, 10 μg/ml each, for 5 min on ice. CR was purified by chromatography on DEAE cellulose, using a NaCl gradient from 0 to 200 mM. Homogeneity was determined with SDS–PAGE [13], using silver staining and Western analysis in parallel.

2.4. Enzymatic assay and kinetic analysis

Kinetic characterization of rat CR and its mutants was determined by following oxidation of NADPH at 340 nm in the presence of varying concentrations of menadione and 4-benzoyl-pyridine with 0.05 mM NADPH in 100 mM phosphate buffer, pH 7.0. K_m and k_{cat} values were determined from Lineweaver–Burk plots.

2.5. Construction of molecular models of rCR1 and rCR2

The template for modeling rCR1 and rCR2 was the 3D structure of pig CR, which has been solved with NADPH [PDB file 1N5D] [14]. The amino acid sequence of pig CR is about 80% identical to that of rCR1 and rCR2. At this degree of sequence identity, the two rCR 3D models will be good representations of the true 3D structure.

Initial 3D models of rCR1 and rCR2 were constructed with the Accelrys Insight II software using the Homology option [15]. To insert menadione into rCR1 and rCR2, we superimposed the initial rCR 3D models with NADPH onto mouse carbonyl reductase [PDB file 1CYD]. The isopropanol substrate was extracted from 1CYD and inserted into rCR1 and rCR2. Then menadione was superimposed onto isopropanol in the four possible orientations and each rCR was minimized using Discover 3 and the CVFF force field for 120 000 iterations.

3. Results and discussion

3.1. Enzymatic activity of rCR1 and rCR2

We compared the catalytic activity of rCR1 and rCR2 for menadione and 4-benzoyl-pyridine. As shown in Table 1, compared to rCR1, rCR2 has a lower K_m towards these substrates. The K_ms of rCR1 for menadione and 4-benzoyl-pyridine are 70 and 1100 μM, respectively. In contrast, the K_ms of rCR2 for menadione and 4-benzoyl-pyridine are 3.3 and 150 μM, respectively. This 20-fold difference between rCR1 and rCR2 in the K_m for menadione was unexpected. Similarly, there are large differences between rCR1 and rCR2 in k_{cat} for menadione and 4-benzoyl-pyridine.

rCR1 and rCR2 differ by only five amino acids in two regions: (a) residues 140, 141, and 143 and (b) residues 235 and 238. To determine the contribution of these amino acids to the differences in catalytic activity of rCR1 and rCR2, we constructed two intermediate mutants, rCR1/2 and rCR2/1. rCR1/2 is identical to rCR1 at positions 140, 141, and 143 and identical to rCR2 at positions 235 and 238. rCR2/1 is identical to rCR1 at positions 235 and 238 and identical to rCR2 at positions 140, 141, and 143.

Table 1
Kinetic constants for testicular and ovarian rat carbonyl reductase and hybrid mutants

Protein	Menadione		4-Benzoyl-pyridine	
	K_m	k_{cat}	K_m	k_{cat}
rCR1	70 μM	4.1	1100 μM	4.75
rCR2/1	350 μM	12.5	1400 μM	14.5
rCR1 A235T	30 μM	4.0	1050 μM	1.4
rCR1 K238E	20 μM	2.0	240 μM	5.6
rCR1/2	3.9 μM	0.9	150 μM	0.85
rCR2	3.3 μM	0.8	150 μM	0.7

rCR2/1 = (rCR1 + G140, M141, R143); rCR1/2 = (rCR1 + T235, E238).

Table 1 summarizes the K_m and k_{cat} of rCR1/2 and rCR2/1 for menadione and 4-benzoyl-pyridine. There are significant differences between these two mutants. The catalytic constants for rCR1/2 are close to those of rCR2, while those for rCR2/1 are higher than those of rCR1. For example, the K_m and kcat of rCR2/1 for menadione are 5-fold and 3-fold higher than those of rCR1. This indicates weaker binding of menadione to rCR2/1, which is consistent with a higher turnover of the substrate.

The closeness of the catalytic constants of rCR1/2 to rCR2 prompted us to look at the individual contributions of the differences at residues at 235 and 238 to the change in catalytic activity. To do this, we constructed two rCR1 mutants, rCR1(A235T) and rCR1(K238E). As shown in Table 1, compared to rCR1, some of the kinetic constants of rCR1(A235T) and rCR1(K238E) are closer to those of rCR2 and some are closer to rCR1. For example, rCR1(K238E) has a K_m for 4-benzyl pyridine that is close to that of rCR2, while kcat for 4-benzoyl-pyridine a little higher than that of rCR1. This indicates that it is combination of the two mutations that is responsible for the differences between rCR1 and rCR2 in reduction of menadione and 4-benzoyl-pyridine.

3.2. Construction and analysis of 3D models of rCR1 and rCR2

To seek clues to the structural basis for the effect of Thr-235 and Glu-238 on substrate binding to rCR2, we constructed 3D models of rCR1 and rCR2 with NADPH and menadione. We superimposed the Cα backbones backbones of rCR1 and rCR2 and find that the RMS difference between their backbones is 0.39 (Fig. 1, Supplement). Upon examination of the overlapped models, we did not find evidence for an allosteric interaction that would influence the catalytic activity of rCR1 and rCR2. As discussed below, the distances between NADPH and the three catalytically important residues: Ser-139, Tyr-193 and Lys-197 [14,16] are consistent with those in pig CR [14] and similar to those found for other SDRs [6,9,14,17–20], which gives us confidence in our 3D models.

Menadione can assume four different orientations in the substrate-binding site in rCR (Fig. 1). It is not clear if more than one of these orientations is suitable for a productive catalytic interaction with tyrosine-193 and NADPH. To resolve this question, we constructed 3D models with menadione in each orientation in rCR1 and rCR2. Both orientations of menadione, in which the quinone is pointing into the interior of the active site of rCR1 and rCR2 (Fig. 2) have favorable distances between the quinone and the catalytically important residues and NADPH. This is consistent with the reduction of ketone, at C1 and C4 of menadione by rCR. Menadione with the quinone pointing away from the catalytic site has less favorable distances to key residues.

Analysis of the 3D models of rCR1 and rCR2 provides an explanation for the stabilizing effects of Thr-235 and Glu-238 in rCR2. As seen in Fig. 2B, in rCR2, Thr-235 Oγ is about 3A from the nicotinamide N7 and O7. Thr-235 Oγ also can interact with the methyl group on menadione. Instead of the hydroxyl side chain of Thr-235, which can form hydrogen bonds with the nicotinamide moiety, Ala-235 of rCR1 has a methyl group as a side chain (Fig. 2A). Thus, Ala-235 is not a hydrogen-bond partner for the nicotinamide group. Moreover, Ala-235 Cβ is about 3.75A from the nicotinamide N7

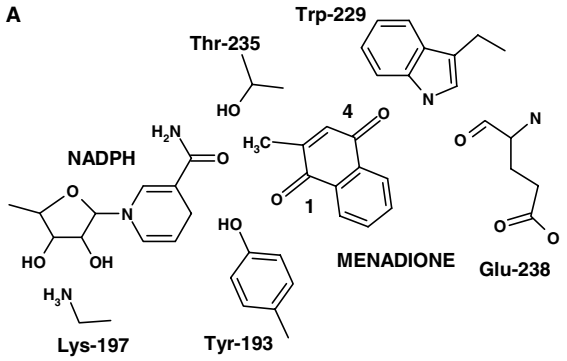

Fig. 1A. Interior orientation of menadione quinone in rCR2 substrate-binding site.

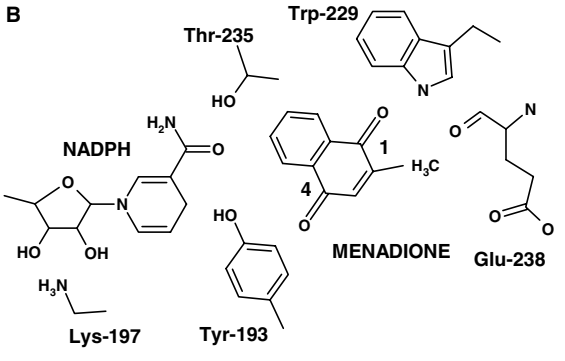

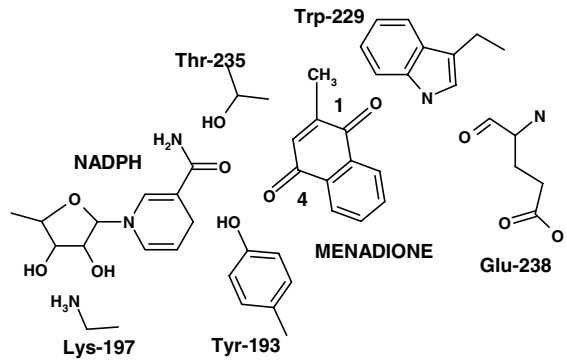

Fig. 1B. Exterior orientation of menadione quinone in rCR2 substrate-binding site.

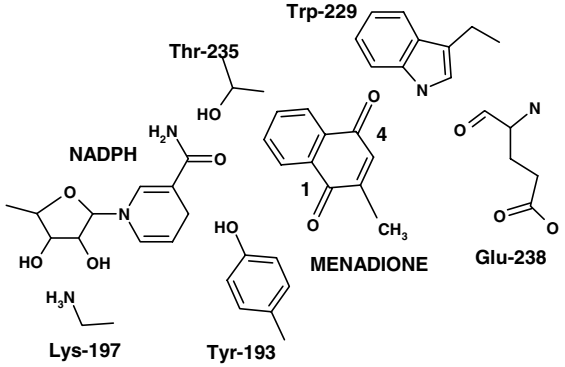

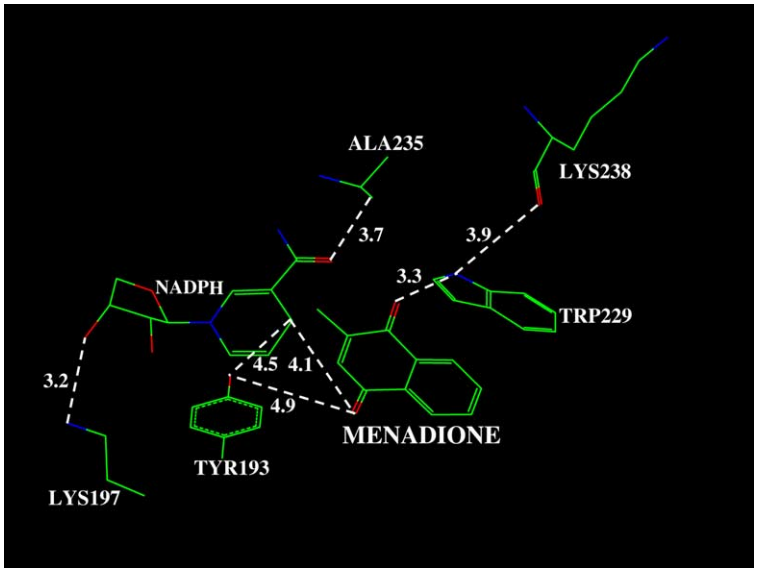

Fig. 2A. Model of Ala-235 and Lys-238 in rCR1.

and O7, and Ala-235 Cβ is too far from the menadione methyl group to influence its position in the substrate-binding site.

Unexpectedly, we found that Glu-238 stabilizes menadione through a relay with Trp-229. As shown in Fig. 2B, the backbone oxygen on Glu-238 is about 3A from Nε1 of Trp-229, which stabilizes the ketone that is not being reduced on menadione. In contrast, the backbone oxygen in Lys-238 in rCR1 is about 4A from Nε1 in Trp-229 (Fig. 2A). This is a weaker interaction with Trp-229.

The 3D model indicates that the residues 140, 141 and 143 of rCR1 of rCR2 appear to perform similar structural functions in each enzyme. In rCR1, Ser-140 interacts with the ketone on menadione that is being reduced (Fig. 2C). Cγ1 of Val-141 is about 4A from this ketone; Cγ2 is about 4A from Cδ2

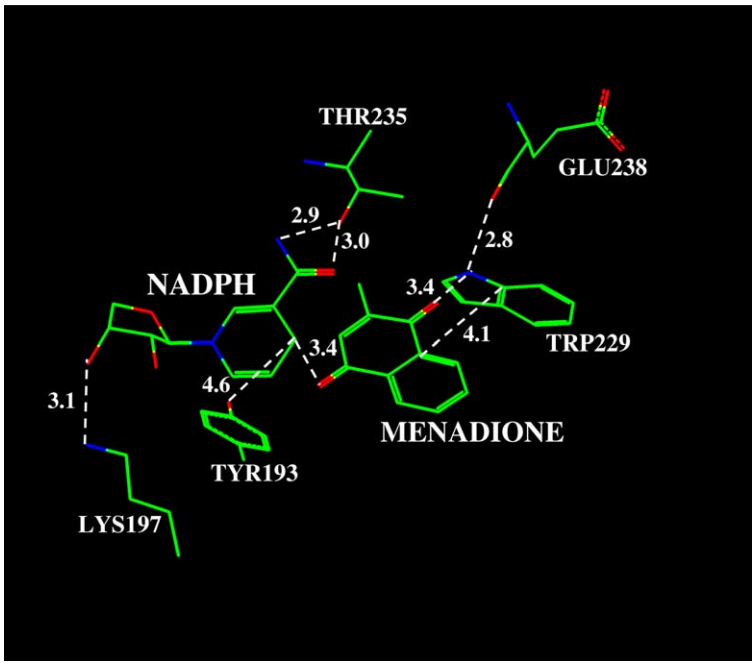

Fig. 2B. Model of Thr-235 and Glu-238 in rCR2.

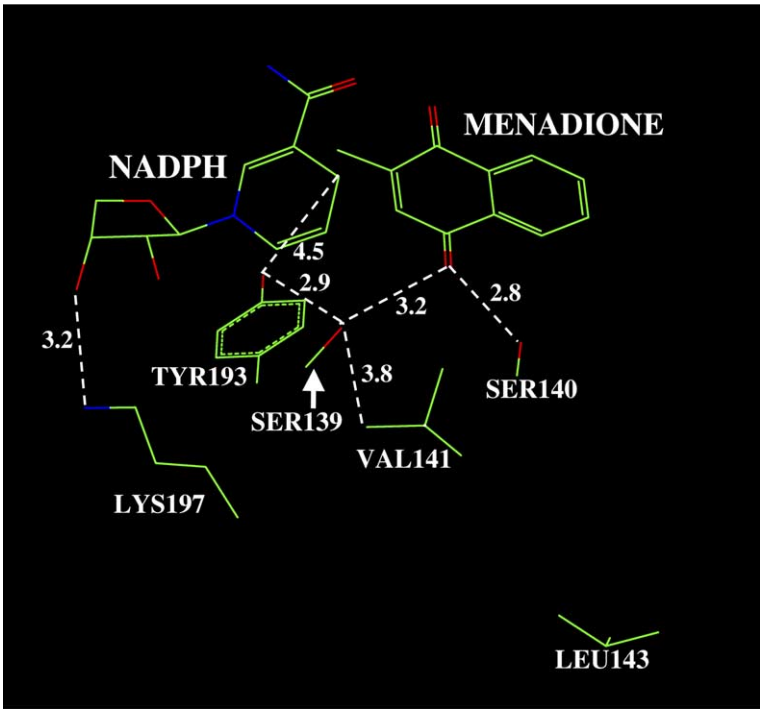

Fig. 2C. Model of Ser-140, Val-141 and Leu-143 in rCR1.

on Tyr-193. Leu-143 does not appear to have important interactions with the substrate or catalytic residues.

In rCR2, Met-141 is about 4A from the ketone on menadione that is reduced (Fig. 2D). Met-141 also interacts with Tyr-193. Arg-143 does not appear to have important interactions with the substrate or catalytic residues.

The 3D models (Figs. 2C and 2D) show that Ser-139 and Tyr-193, which is part of the catalytic triad of CR [6,14,16] are farther from each other in rCR2 than in rCR1. This may explain the increased K_m found in rCR2/1.

rCR2 is unique among mammalian CRs in having an amino acid at 235 with an alcohol side chain and an amino acid at 238

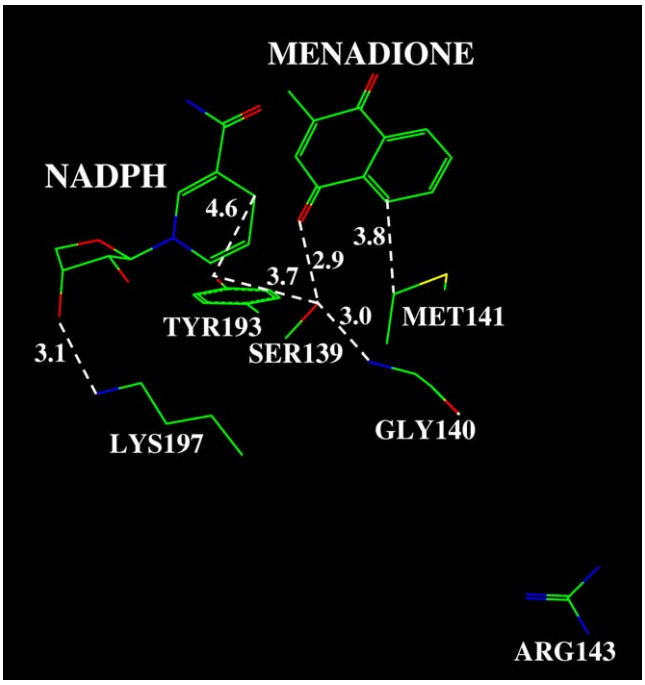

Fig. 2D. Model of Gly-140, Met-141 and Arg-143 in rCR2.

Rat CR1	**232**	T	D	M	A	G	P	K	A	T	K	S	P	E	E	**245**
Rat CR2	**232**	T	D	M	T	G	P	E	A	T	K	S	P	E	E	**245**
Hu man CR	**232**	T	D	M	A	G	P	K	A	T	K	S	P	E	E	**245**
Mou se CR	**232**	T	D	M	A	G	P	K	A	T	K	S	P	E	E	**245**
Pig CR	**232**	T	D	M	G	G	P	K	A	P	K	S	P	E	V	**245**
Rabbit CR	**232**	T	D	M	G	G	P	N	A	T	K	S	P	E	E	**245**

Fig. 3. Alignment of several carbonyl reductases near residues 235 and 238.

with a negatively charged side chain. As shown in Fig. 3, human CR and mouse CR have alanine-235 and lysine-238 [15]. Pig CR has a glycine-235. Rabbit CR has glycine-235 and asparagine-238. The two apparently small evolutionary changes in rCR2 increase its affinity for menadione (Table 1). Our data raise the intriguing possibility that differences in positions 235 and 238 in other CRs may be functionally important.

Acknowledgments: We thank Elsbeth Ernst and Micheline Schaller for expert technical assistance and C. Chandsawangbhuwana for help with 3D figures. This work was supported by joint contributions of European Community Biotech 2 program (Bio4 CT972123) and the Swiss Federal Office of Education and Science (97-0153).

References

[1] Wermuth, B. (1981) Purification and properties of an NADPH-dependent carbonyl reductase from human brain: relationship to prostaglandin 9-keto reductase and xenobiotic ketone reductase. J. Biol. Chem. 256, 1206–1213.
[2] Wermuth, B., Bohren, K.M., Heinemann, G., von Wartburg, J.P. and Gabbay, K.H. (1988) Human carbonyl reductase: nucleotide sequence analysis and amino acid sequence of the encoded protein. J. Biol. Chem. 263, 16185–16188.
[3] Watanabe, K., Sugawara, C., Ono, A., Fukuzumi, Y., Itakura, S., Yamazaki, M., Tashiro, H., Osoegawa, K., Soeda, E. and Nomura, T. (1998) Mapping of a novel human carbonyl reductase, CBR3, and ribosomal pseudogenes to human chromosome 21q22.2. Genomics 52, 95–100.
[4] Wermuth, B., Bohren, K. and Ernst, E. (1993) Autocatalytic modification of human carbonyl reductase by 2-oxocarboxylic acids. FEBS Lett. 335, 151–154.
[5] Aoki, H., Okada, T., Mizutani, T., Numata, Y., Minegishi, T. and Miyamoto, K. (1997) Identification of two closely related genes, inducible and noninducible carbonyl reductases in the rat ovary. Biochem. Biophys. Res. Commun. 230, 518–523.
[6] Jornvall, H., Persson, B., Krook, M., Atrian, S., Gonzalez-Duarte, R., Jeffrey, J. and Ghosh, D. (1995) Short-chain dehydrogenases/reductases (SDR). Biochemistry 34, 6003–6013.
[7] Baker, M.E. (2001) Evolution of 17beta-hydroxysteroid dehydrogenases and their role in androgen, estrogen and retinoid action. Mol. Cell. Endocrinol. 171, 211–215.
[8] Wermuth, B., Mäder-Heineman, G. and Ernst, E. (1995) Cloning and expression of carbonyl reductase from rat testis. Eur. J. Biochem. 228, 473–479.
[9] Tanaka, N., Nonaka, T., Tanabe, T., Yoshimoto, T., Tsuru, D. and Mitsui, Y. (1996) Crystal structures of the binary and ternary complexes of 7α-hydroxysteroid dehydrogenase from *Escherichia coli*. Biochemistry 35, 7715–7730.
[10] Krook, M., Ghosh, D., Strömberg, R., Carlquist, M. and Jornvall, H. (1993) Carboxyethyllysine in a protein: native carboxy reductase/NADP$^+$-dependent prostaglandin dehydrogenase. Proc. Natl. Acad. Sci. USA 90, 502–506.
[11] Sciotti, M.A., Nakajin, S., Wermuth, B. and Baker, M.E. (2000) Mutation of threonine-241 to proline eliminates autocatalytic modification of human carbonyl reductase. Biochem. J. 350, 89–92.
[12] Higuchi, R., Krummel, B. and Saiki, R.K. (1988) A general method of in vitro preparation and specific mutagenesis of DNA fragments: study of protein and DNA interactions. Nucleic Acids Res. 16, 7351–7367.
[13] Laemmli, U.K. (1970) Cleavage of structural proteins during the assembly of the head of bacteriophage T_4. Nature 27, 680–685.
[14] Ghosh, D., Sawicki, M., Pletnev, V., Erman, M., Ohno, S., Nakajin, S. and Duax, W.L. (2001) Porcine carbonyl reductase. structural basis for a functional monomer in short chain dehydrogenases/reductases. J. Biol. Chem. 276, 18457–18463.
[15] Homology, User Manual, Accelrys Inc. San Diego, 1998..
[16] Nakajin, S., Takase, N., Ohno, S., Toyoshima, S. and Baker, M.E. (1998) Mutation of tyrosine-194 and lysine-198 in the catalytic site of pig 3α/β,20β-hydroxysteroid dehydrogenase. Biochem. J. 334, 553–557.
[17] Yamashita, A., Kato, H., Wakatsuki, S., Tomiyaki, T., Nakatsu, T., Nakajima, K., Hashimoto, T., Yamada, Y. and Oda, J. (1999) Structure of tropinone reductase-II complexed with NADP$^+$ and pseudotropine at 1.9 AA resolution: implication for sterospecific substrate binding and catalysis. Biochemistry 38, 7630–7637.
[18] Benach, J., Atrian, S., Gonzalez-Duarte, R. and Ladenstein, R. (1998) The refined crystal structure of *Drosophila lebanonensis* alcohol dehydrogenase at 1.9 Å resolution. J. Mol. Biol. 282, 383–399.
[19] Breton, R., Housset, D., Mazza, C. and Fontecilla-Camps, J.C. (1996) The structure of a complex of human 17β-hydroxysteroid dehydrogenase with estradiol and NADP$^+$ identifies two principal targets for the design of inhibitors. Structure 4, 905–915.
[20] Sawicki, M.W., Erman, M., Puranen, T., Vihko, P. and Ghosh, D. (1999) Structure of the ternary complex of human 17-hydroxysteroid dehydrogenase type 1 with 3-hydroxyestra-1,3,5,7-tetraen-17-one (equilin) and NADP$^+$. Proc. Natl. Acad. Sci. USA 96, 840–845.